Supplement of Biogeosciences, 17, 3961–3989, 2020
https://doi.org/10.5194/bg-17-3961-2020-supplement

Biogeosciences Open Access EGU

Supplement of

Understanding the uncertainty in global forest carbon turnover

Thomas A. M. Pugh et al.

Correspondence to: Thomas A. M. Pugh (t.a.m.pugh@bham.ac.uk)

Table S1. Plant functional types (PFTs) simulated by each terrestrial biosphere model (TBM) and their grouping into forest-type classifications.

Forest-type classifications	TBM PFTs (forest-type classification in parentheses)					
	CABLE-POP	**JULES**	**LPJ-GUESS**	**LPJmL**	**ORCHIDEE**	**SEIB-DGVM**
Tropical broadleaved deciduous (TrBD)	Deciduous broadleaf forest (TrBD, TeBD, BBD[a])	Broadleaf deciduous tree (TrBD, TeBD, BBD[a])	Tropical broadleaf raingreen tree (TrBD)	Tropical broad-leaved raingreen tree (TrBD)	Tropical broad-leaved raingreen tree (TrBD)	Tropical broad-leaved raingreen tree (TrBD)
Tropical broadleaved evergreen (TrBE)	Evergreen broadleaf forest (TrBE, TeBE[a])	Tropical broadleaved evergreen tree (TrBE)	Tropical broadleaf evergreen tree (TrBE)[b]	Tropical broad-leaved evergreen tree (TrBE)	Tropical broad-leaved evergreen tree (TrBE)	Tropical broad-leaved evergreen tree (TrBE)
Temperate broadleaved deciduous (TeBD)	Deciduous broadleaf forest (TrBD, TeBD, BBD[a])	Broadleaf deciduous tree (TrBD, TeBD, BBD[a])	Temperate broadleaf summergreen tree (TeBD, BBD)[b]	Temperate broad-leaved summergreen tree (TeBD)	Temperate broad-leaved summergreen tree (TeBD)	Temperate broad-leaved summergreen tree (TeBD)
Temperate broadleaved evergreen (TeBE)	Evergreen broadleaf forest (TrBE, TeBE[a])	Temperate broadleaved evergreen tree (TeBE)	Temperate broadleaf evergreen tree (TeBE)	Temperate broad-leaved evergreen tree (TeBE)	Temperate broad-leaved evergreen tree (TeBE)	Temperate broad-leaved evergreen tree (TeBE)
Boreal broadleaved deciduous (BBD)	Deciduous broadleaf forest (TrBD, TeBD, BBD[a])	Broadleaf deciduous tree (TrBD, TeBD, BBD[a])	NA[c]	Boreal broad-leaved summergreen tree (BBD)	Boreal broad-leaved summergreen tree (BBD)	Boreal broad-leaved summergreen tree (BBD)
Needleleaved deciduous (ND)	Deciduous needleleaf forest (ND)	Needleleaf deciduous tree (ND)	Boreal needleleaf summergreen tree (ND)	NA[c]	Boreal needleleaf summergreen tree (ND)	Boreal needle-leaved summergreen tree (ND)
Needleleaved evergreen (NE)	Evergreen needleleaf forest (NE)	Needleleaf evergreen tree (NE)	Boreal needleleaf evergreen tree (NE)[b]	Temperate needle-leaved evergreen tree (NE) Boreal needle-leaved evergreen tree (NE)	Temperate needleleaf evergreen tree (NE) Boreal needleleaf evergreeen tree (NE)	Temperate needle-leaved evergreen tree (NE) Boreal needle-leaved evergreen tree (NE)
Non-forest (NF), shrub	Shrub (NF)	Deciduous shrub (NF) Evergreen shrub (NF)	NA[c]	NA[c]	NA[c]	NA[c]
Non-forest (NF), herbaceous	C3 grass (NF) C4 grass (NF)	C3 grass (NF) C4 grass (NF)	C3 grasses (NF) C4 grasses (NF)	Tropical herbaceous (NF) Temperate herbaceous (NF)	C3 grass (NF) C4 grass (NF)	Tropical herbaceous (NF) Temperate herbaceous (NF)

[a] PFT assigned to more than one forest type: tropical forest when latitude is between 23° N and 23° S, temperate forest when latitude is >23° N to ≤55° N or >23° S, and boreal forest when latitude is >55° N.
[b] Both shade-tolerant and shade intolerant PFTs simulated.
[c] PFT not simulated for this study.

Table S2. Phenological longevity parameters (years) in the terrestrial biosphere model (TBM) ensemble.

Forest type[c]	Model											
	CABLE-POP		JULES		LPJ-GUESS		LPJmL		ORCHIDEE		SEIB-DGVM	
	Leaf	Root[d]	Leaf	Root[d]	Leaf	Root[d]	Leaf	Root[d]	Leaf	Root[d]	Leaf	Root[d]
Boreal needleleaved deciduous	0.52	0.7	1.0[a]	6.67	1.0[b]	1.4	1.0	1.0	1.0[b]	1.0[b]	1.0[b]	5.0
Boreal needleleaved evergreen	3.5	0.7	4.0[a]	6.67	3.0	1.4	2.0	2.0	3.0	3.0	4.55	2.38
Boreal broadleaved deciduous	n/a	n/a	n/a	n/a	n/a	n/a	1.0	1.0	1.0[b]	1.0[b]	1.0[b]	2.13
Temperate needleleaved evergreen	3.5	0.7	n/a	n/a	n/a	n/a	2.0	2.0	3.0	3.0	4.55	1.56
Temperate broadleaved evergreen	3.5	0.7	2.0[a]	4.0	3.0	1.4	1.0	1.0	1.0	1.0	2.63	1.56
Temperate broadleaved deciduous	2	0.7	1.0[a]	4.0	1.0[b]	1.4	1.0	1.0	1.0[b]	1.0[b]	1.0[b]	1.56
Tropical broadleaved evergreen	3.5	0.7	4.0[a]	4.0	2.0	1.4	2.0	2.0	2.5	2.5	1.69	1.32
Tropical broadleaved deciduous	n/a	n/a	1.0[a]	4.0	1.0[b]	1.4	1.0	1.0	1.0[b]	1.0[b]	1.0[b]	0.63
C3 herb	0.5	0.29	0.33	4.0	1.0	1.4	1.0	2.0	0.5	0.5	2.0	2.50
C4 herb	0.5	0.21	0.33	4.0	1.0	1.4	1.0	2.0	0.5	0.5	2.0	1.3

[a] JULES modifies phenology on a baseline turnover rate according to if the ambient temperature dips below a defined leaf-off temperature. The values in this table assume that the leaf-off temperature is never achieved for evergreen trees, but is achieved every year for deciduous trees.
[b] Reported here as one for deciduous phenologies on the assumption that only one leaf flush per year will be permitted. Actual leaf longevity is shorter.
[c] Where forest-type classifications cover multiple PFTs, the most representative PFT is listed.
[d] All root values are reported for fine roots only.

Table S3. Mapping of European Space Agency (ESA) landcover classes to forest types used in this analysis.

Code	Forest-type classification	ESA landcover classes[1]	Additional conditions
TrBE	Tropical broadleaved evergreen	50	latitude ≤ 23°
TrBD	Tropical broadleaved deciduous	60, 61, 62	latitude ≤ 23°
OTr	Other tropical forest	100, 160, 170	latitude ≤ 23°
TeBE	Temperate broadleaved evergreen	50	latitude > 23°
TeBD	Temperate broadleaved deciduous	60, 61, 62	latitude > 23°
NE	Needleleaved evergreen	70, 71, 72	n/a
ND	Needleleaved deciduous	80, 81, 82	n/a
MX	Broadleaved-needleleaved mixed forest	90	n/a
Other	Other forest	100, 160, 170	latitude > 23°

[1]ESA (2017), Pugh et al. (2019b)

Table S4. Leaf area to sapwood area ratios used in the terrestrial biosphere model (TBM) ensemble

PFT type[a]	LA:SA (m^2 cm^{-2})					
	CABLE-POP	**JULES**	**LPJ-GUESS**	**LPJmL**	**ORCHIDEE**	**SEIB-DGVM**
Boreal needleleaved deciduous	4000	[b]	5000	8000	no constraint	6000
Boreal needleleaved evergreen	4000	[b]	5000	8000	no constraint	6000
Boreal broadleaved deciduous	4000	n/a	n/a	n/a	n/a	8500
Temperate needleleaved evergreen	4000	n/a	n/a	8000	no constraint	4800
Temperate broadleaved evergreen	4000	[b]	6000	8000	no constraint	4800
Temperate broadleaved deciduous	4000	[b]	6000	8000	no constraint	14500
Tropical broadleaved evergreen	4000	[b]	6000	8000	no constraint	no constraint
Tropical broadleaved deciduous	4000	[b]	6000	8000	no constraint	no constraint

[a] Where forest-type classifications cover multiple PFTs, the value for the most representative PFT is listed.
[b] JULES does not define an area ratio, but instead relates leaf area to mass of sapwood for the purpose of calculating respiration (Eq. 46 in Clark et al., 2011).

Table S5. Performance of terrestrial biosphere models (TBMs) in capturing observed drought-induced mortality events.

Model	N[1]	Fraction of observed drought-induced events with increased mortality				
		All mechanisms		Most drought-sensitive relevant process		
		Drought period + 5 years	Random[2]	Drought period + 5 years	Random	Process-type (Table 3)
CABLE-POP	25	0.08	0.03	0.12	0.02	Growth efficiency
JULES	25	0.16	0.04	0.16	0.12	Self-thinning
LPJ-GUESS	26	0.04	0.02	0.12	0.04	Growth efficiency
LPJmL	19	0.11	0.05	0.11	0.03	Self-thinning
ORCHIDEE	22	0.05	0.04	n/a	n/a	n/a
SEIB-DGVM	25	0.04	0.04	0.27	0.04	Bioclimatic limits

[1] Total number of events for which the model simulated forest and a mortality flux was recorded in at least one year during the period 1901-2015.
[2] Mean of 10 randomly selected year ranges.

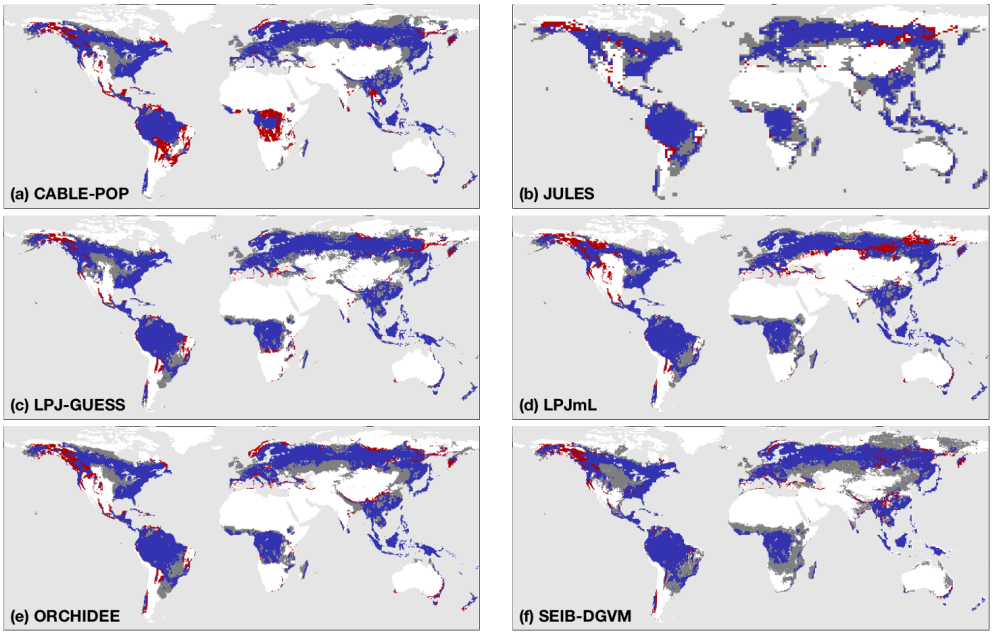

Figure S1. Evaluation of grid-cells where TBMs simulate forest for the period 1985-2014 (see Methods for definition) against satellite observations for the year 2000 (Hansen et al., 2013). Blue shading indicates where the TBM simulates forest and satellite observations find at least 10% of the grid-cell to be covered by forest with a 50% canopy-cover threshold (Pugh et al., 2019a). Red shading indicates where forest is observed in the satellite data but not simulated by the TBM. Grey shading indicates where forest is simulated by the TBM but is not observed in the satellite data.

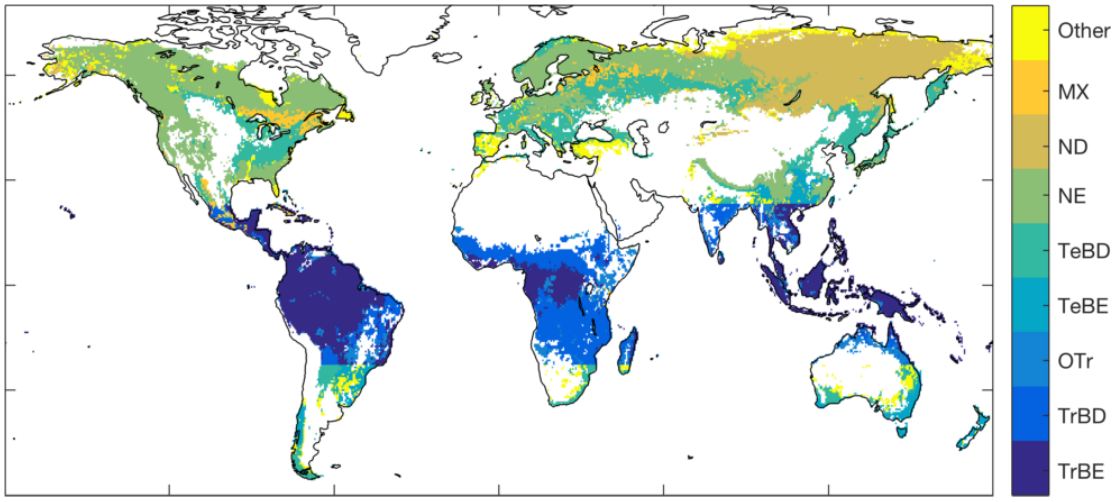

Figure S2. Forest type regions based on the European Space Agency (ESA) land-cover map (ESA 2017). Reproduced from Pugh et al. (2019b), Fig. S9. See Table S3 for forest type codes.

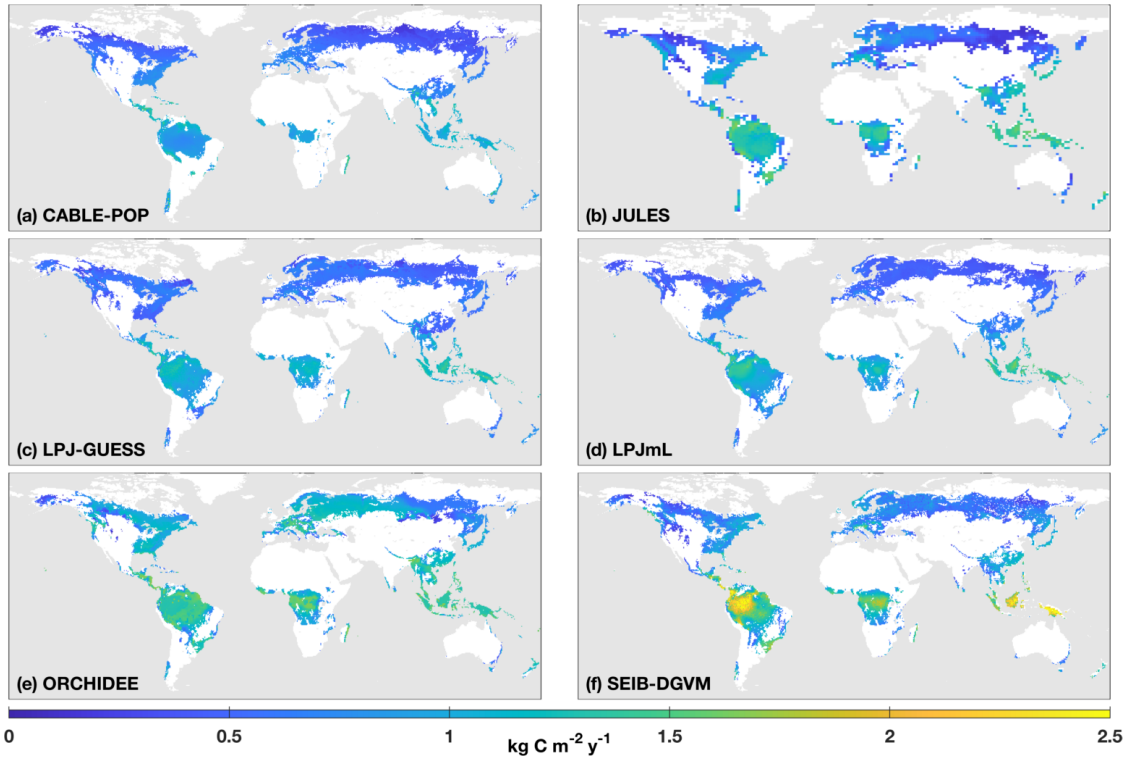

Figure S3. NPP mean for the period 1985-2014 as forced by the CRU-NCEP climate (units of kg C m^{-2} y^{-1}). Colour scale is capped at 2.5 kg C m^{-2} y^{-1}. Maps show areas which are simulated as forest for each model and have at least 10% of the grid-cell covered by closed-canopy forest (see Methods).

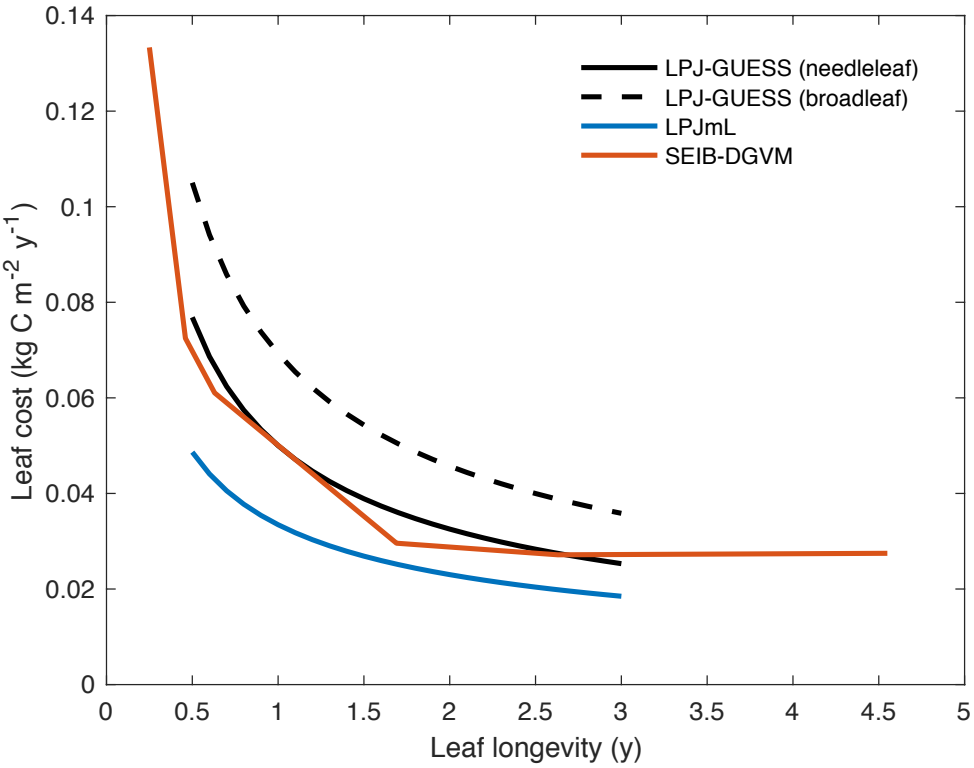

Figure S4. Leaf C cost as a function of longevity for three of the TBMs. Leaf C cost is defined as the reciprocal of specific leaf area divided by leaf longevity.

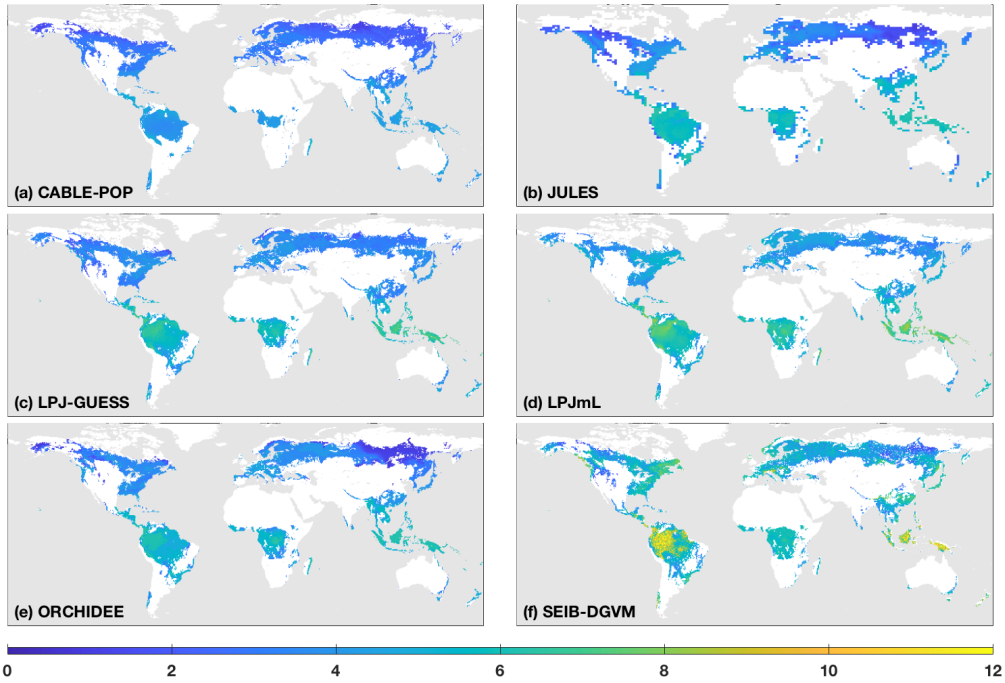

Figure S5. Annual mean maximum value of the monthly LAI (m^2 m^{-2}) over the period 1985-2014 in the CRU-NCEP-forced simulation.

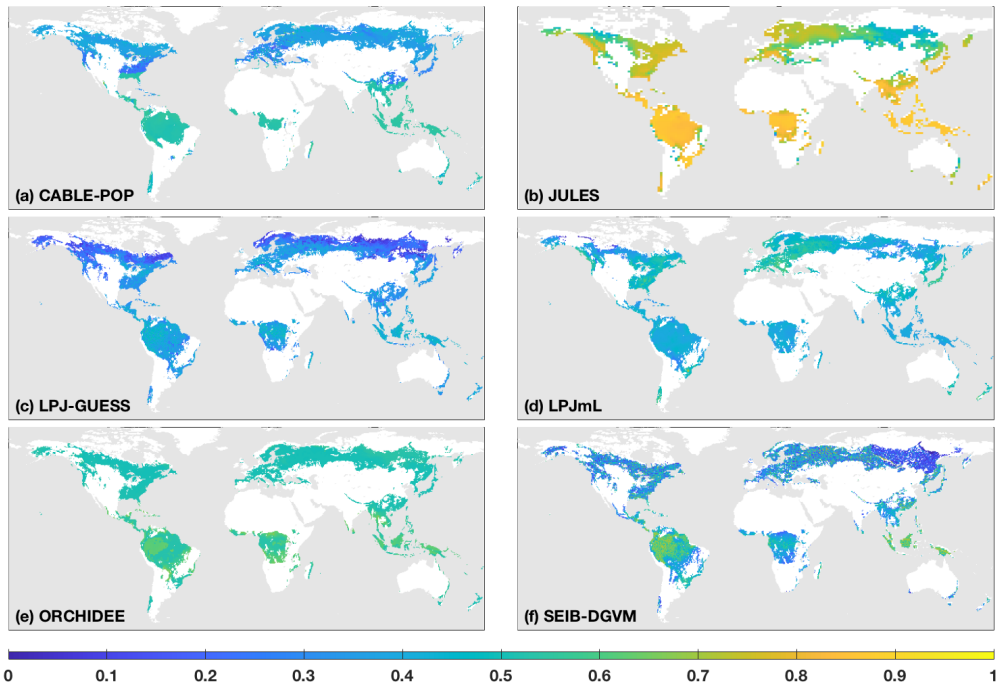

Figure S6. Fraction of F_{turn} which results from mortality (F_{mort} / F_{turn}), for the period 1985-2014 as forced by the CRU-NCEP climate. The fraction of F_{turn} resulting from phenological processes is the remainder. Masking as for Fig. 1.

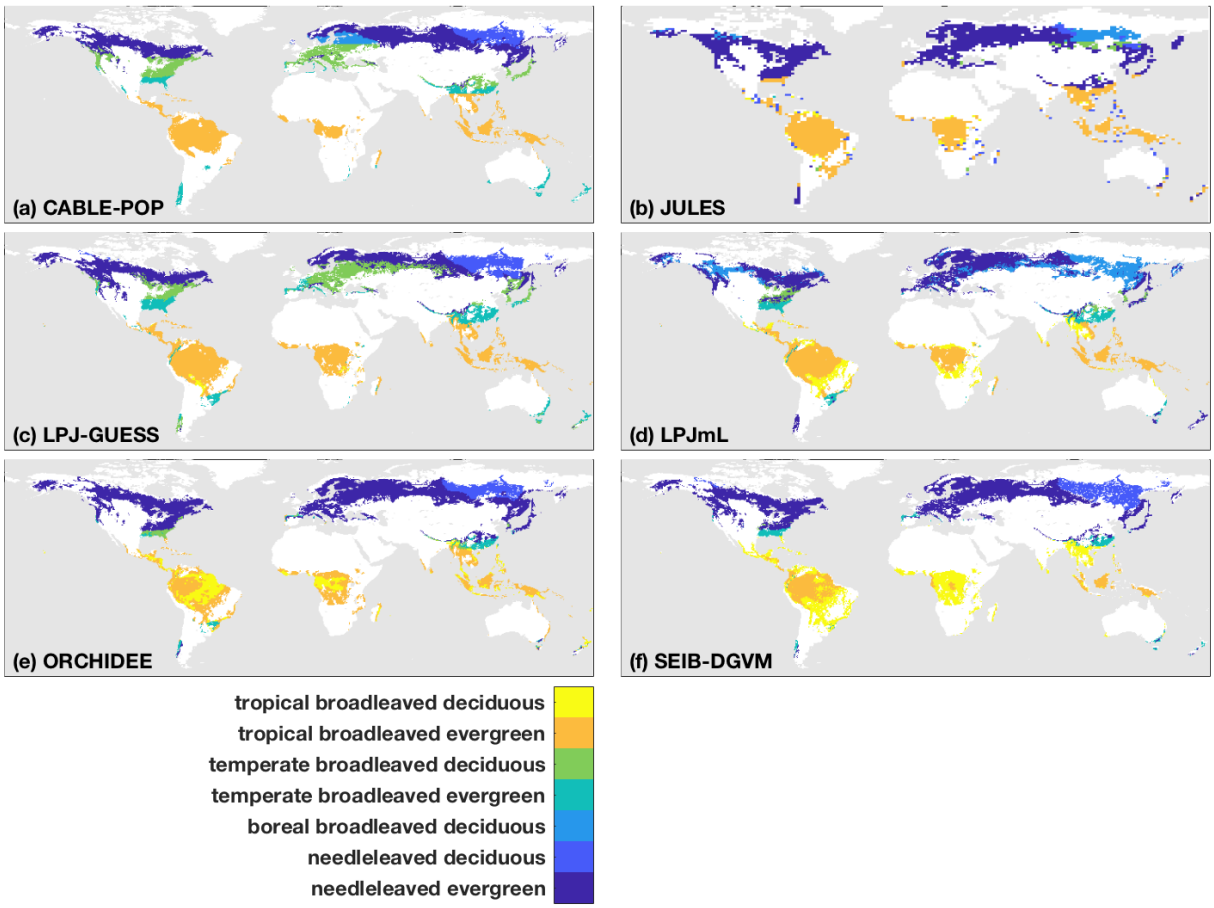

Figure S7. Distribution of the model simulated forest types during 1985-2014 based on the CRU-NCEP simulation.

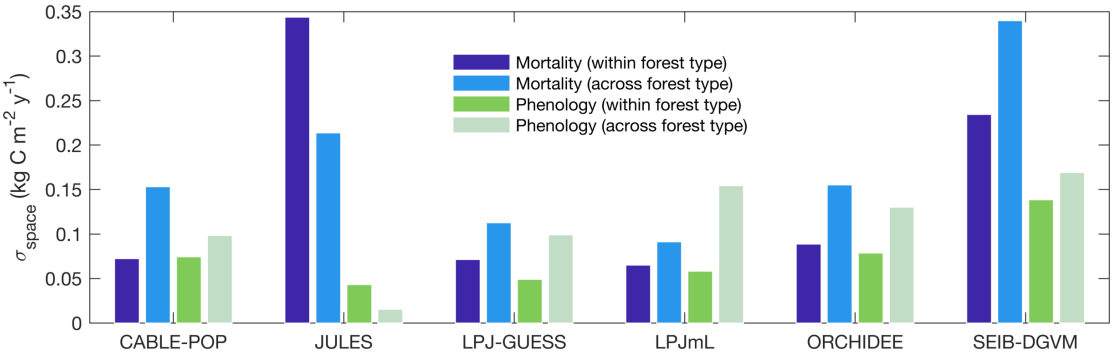

Figure S8. Standard deviation of turnover fluxes in space for F_{mort} and F_{phen}, calculated by model forest types over the period 1985-2014 from the CRU-NCEP-forced simulation. For "within forest type" variance was calculated for each forest type, before taking the square root of the mean variance across all forest types. For "across forest type" the mean of fluxes across each forest type was taken, before calculating the standard deviation of these forest-type means. Calculations were only made across grid-cells with at least 10% forest cover. Comparisons of absolute numbers from JULES with those of other TBMs should be avoided because of the different spatial resolution.

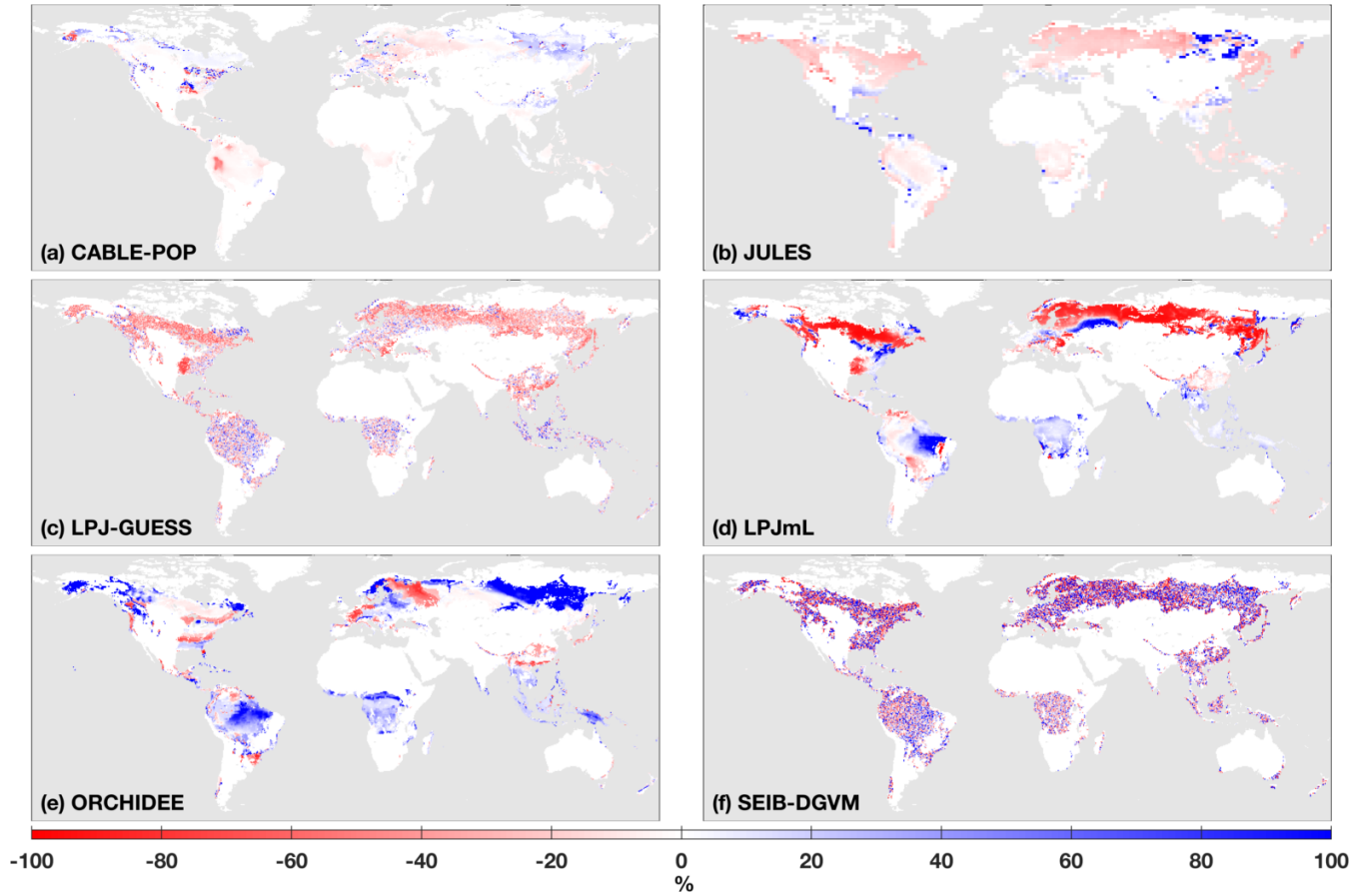

Figure S9. Percentage change in τ_{mort} (C_{veg}/F_{mort}) mean between the periods 1985-2014 and 2070-2099 as forced by the IPSL-CM5A-LR climate (units of years). Masking as for Fig. 1.

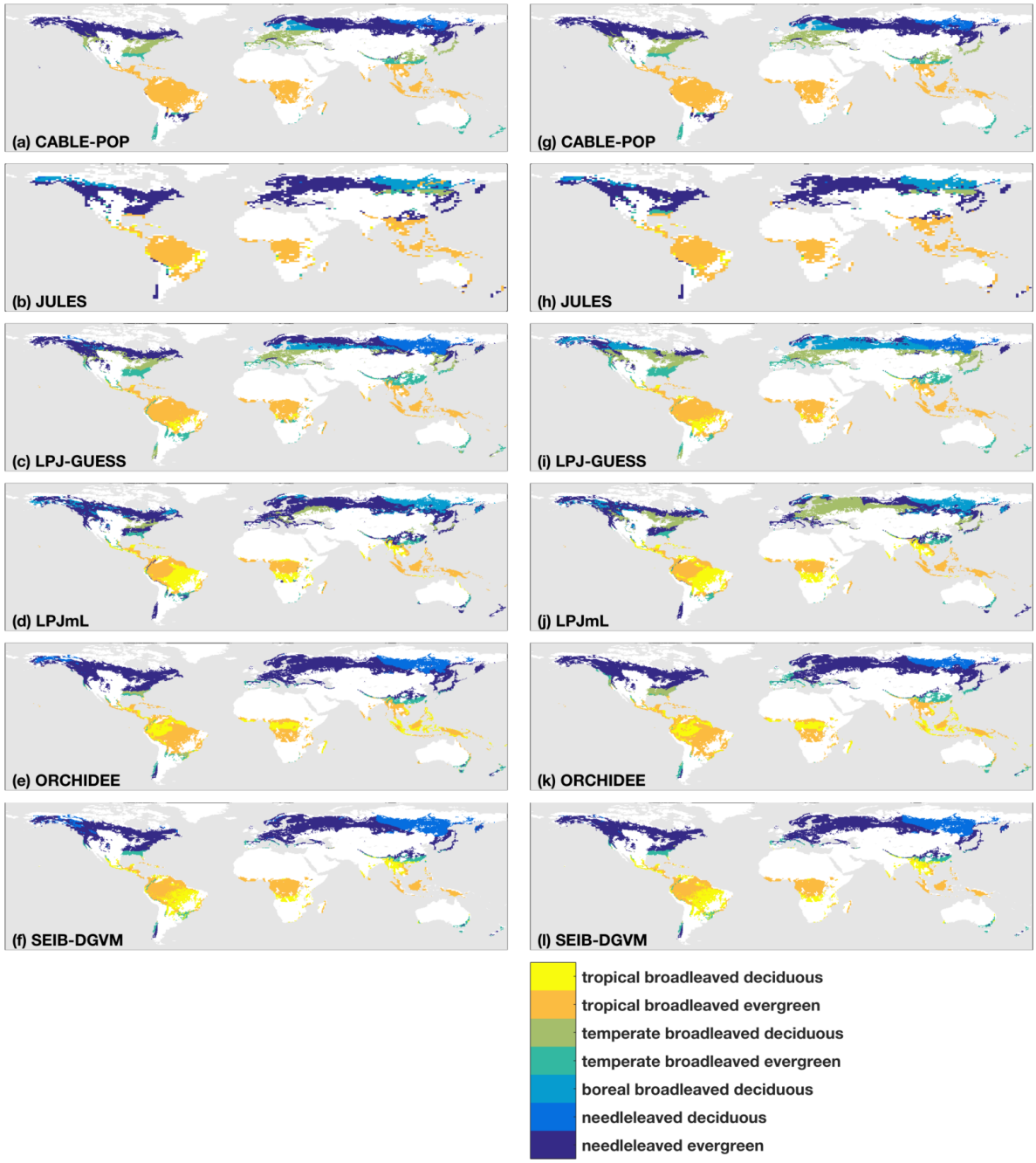

Figure S10. Distribution of the model simulated forest types during 1985-2014 (a-f) and 2070-2099 (g-l) in the TBM simulations forced by IPSL-CM5A-LR RCP 8.5 bias-corrected climate data.

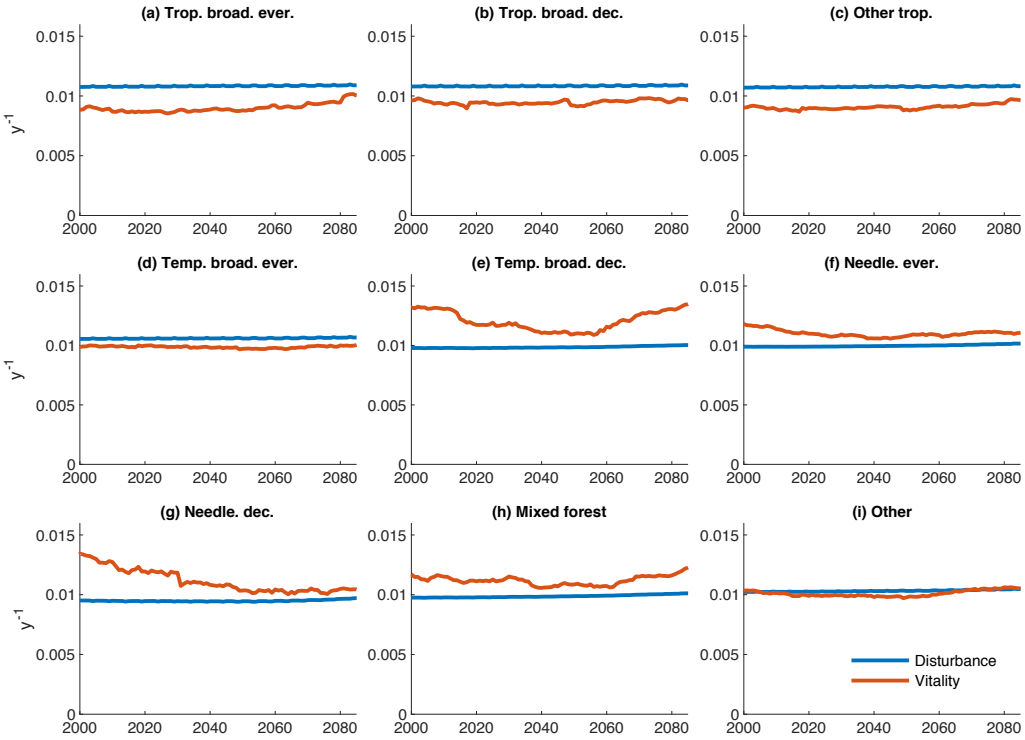

Figure S11. Mortality rate (F_{mort}/C_{veg}) for CABLE-POP split by conceptual process grouping (Table 3) and observational forest type for 1985-2099 in the simulation forced by IPSL-CM5A-LR RCP 8.5 bias-corrected climate data. 31-year running means are plotted for clarity and thus only 2000-2085 is shown. Rates are calculated based on grid-cell total C_{veg} and mortality fluxes.

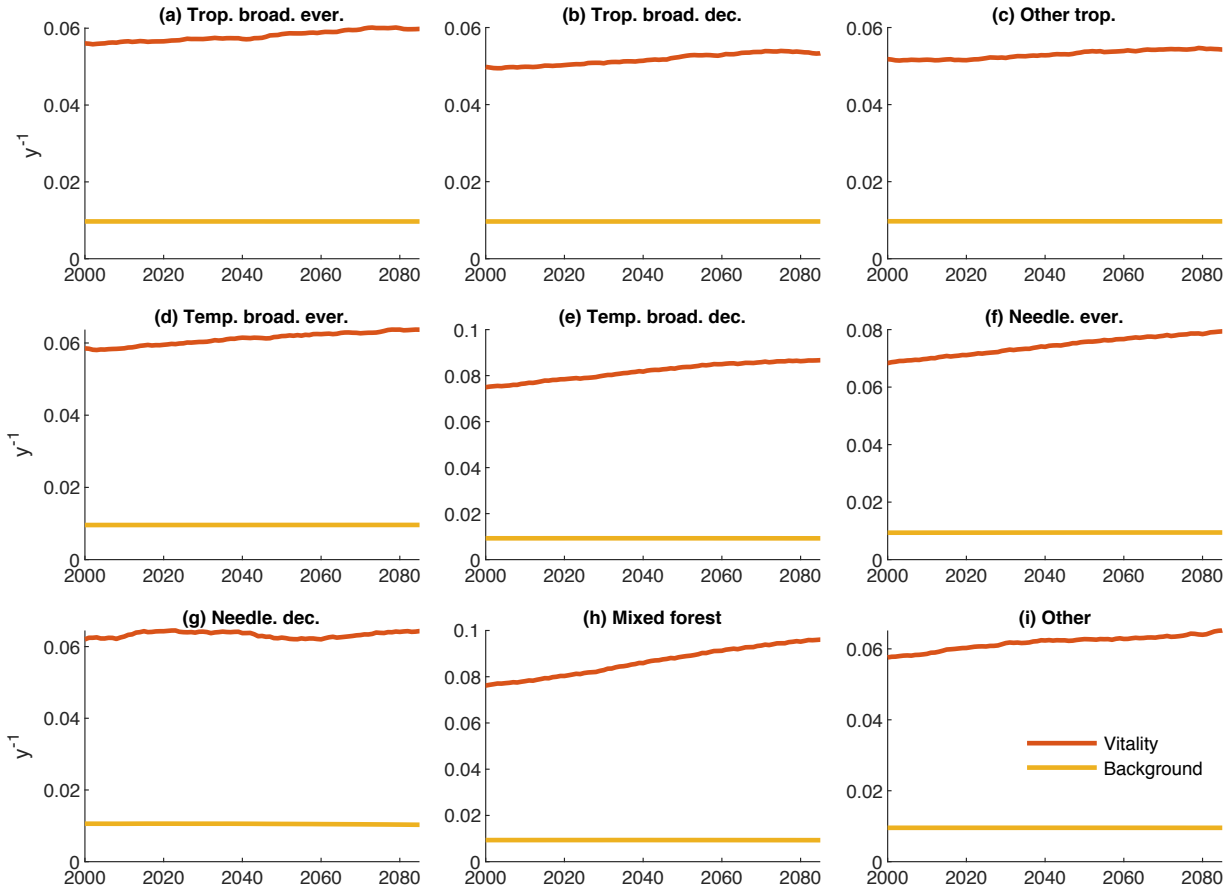

Figure S12. Mortality rate (F_{mort}/C_{veg}) for JULES split by conceptual process grouping (Table 3) and observational forest type for 1985-2099 in the simulation forced by IPSL-CM5A-LR RCP 8.5 bias-corrected climate data. 31-year running means are plotted for clarity and thus only 2000-2085 is shown. Rates are calculated based on grid-cell total C_{veg} and mortality fluxes.

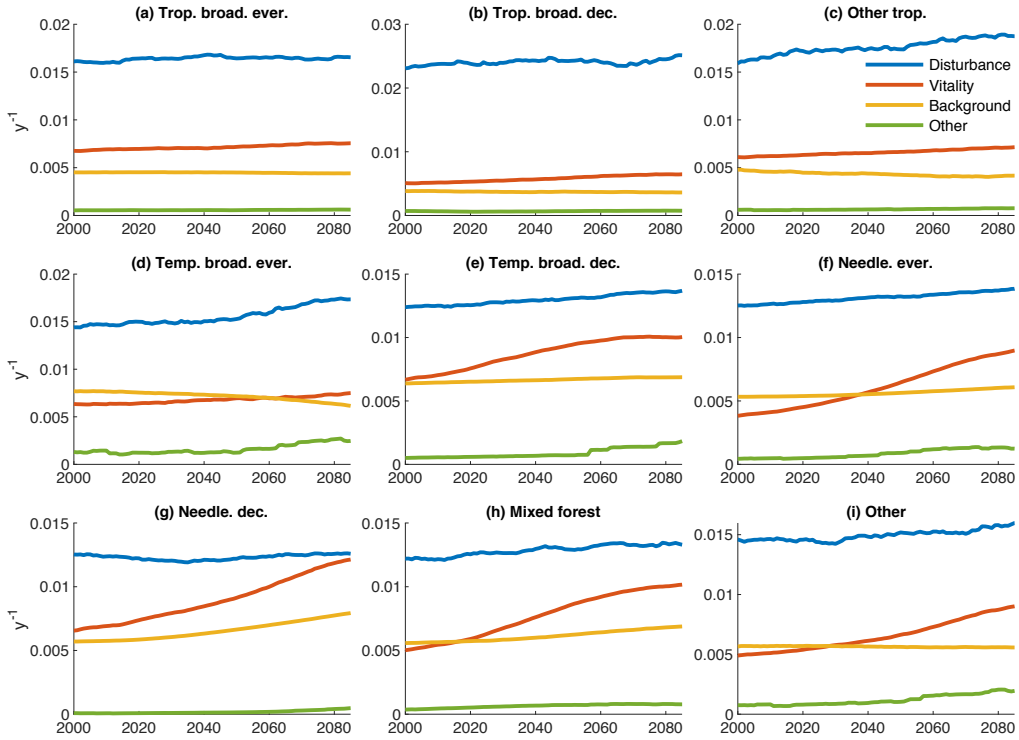

Figure S13. Mortality rate (F_{mort}/C_{veg}) for LPJ-GUESS split by conceptual process grouping (Table 3) and observational forest type for 1985-2099 in the simulation forced by IPSL-CM5A-LR RCP 8.5 bias-corrected climate data. 31-year running means are plotted for clarity and thus only 2000-2085 is shown. Rates are calculated based on grid-cell total C_{veg} and mortality fluxes.

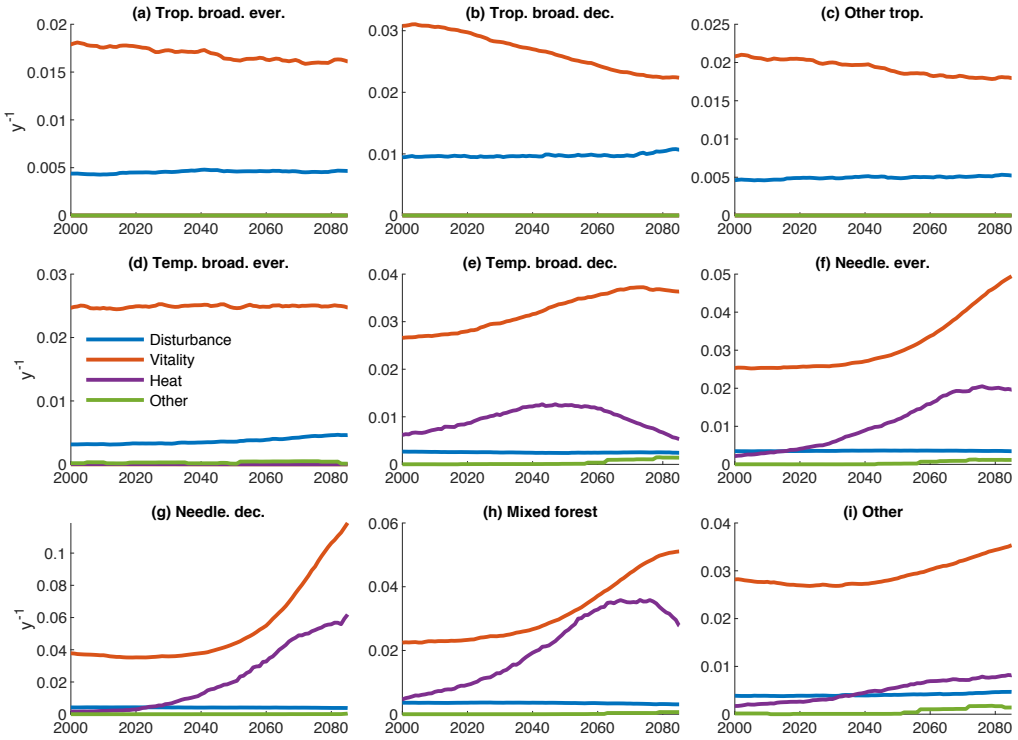

Figure S14. Mortality rate (F_{mort}/C_{veg}) for LPJmL split by conceptual process grouping (Table 3) and observational forest type for 1985-2099 in the simulation forced by IPSL-CM5A-LR RCP 8.5 bias-corrected climate data. 31-year running means are plotted for clarity and thus only 2000-2085 is shown. Rates are calculated based on grid-cell total C_{veg} and mortality fluxes.

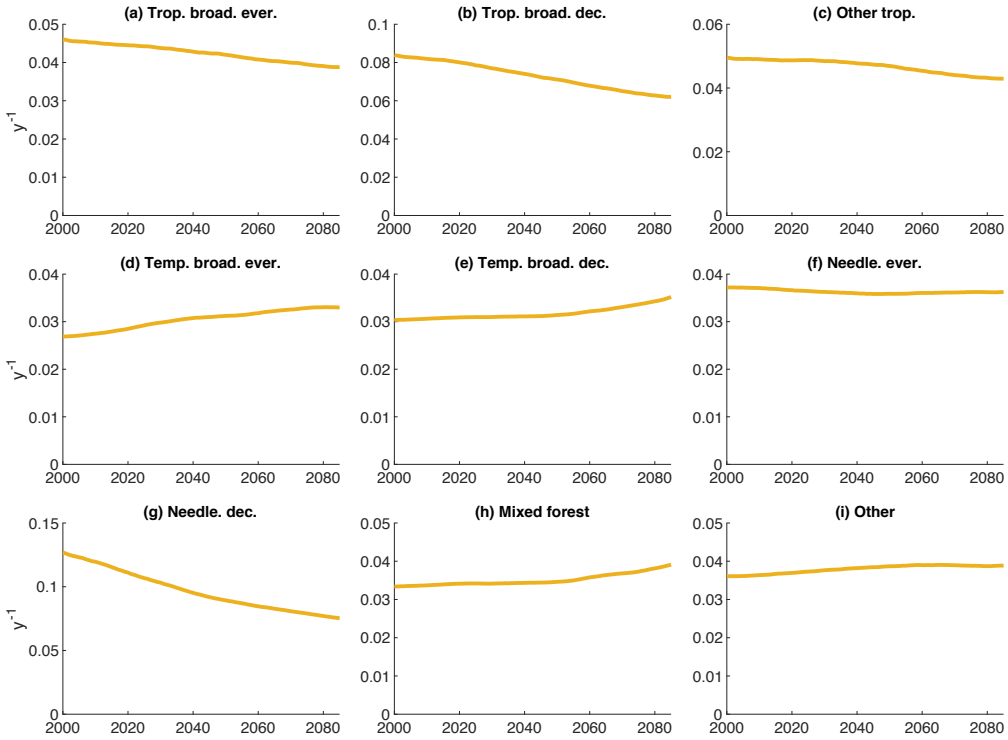

Figure S15. Mortality rate (F_{mort}/C_{veg}) for ORCHIDEE split by observational forest type for 1985-2099 in the simulation forced by IPSL-CM5A-LR RCP 8.5 bias-corrected climate data. No mechanism breakdown was available. 31-year running means are plotted for clarity and thus only 2000-2085 is shown. Rates are calculated based on grid-cell total C_{veg} and mortality fluxes.

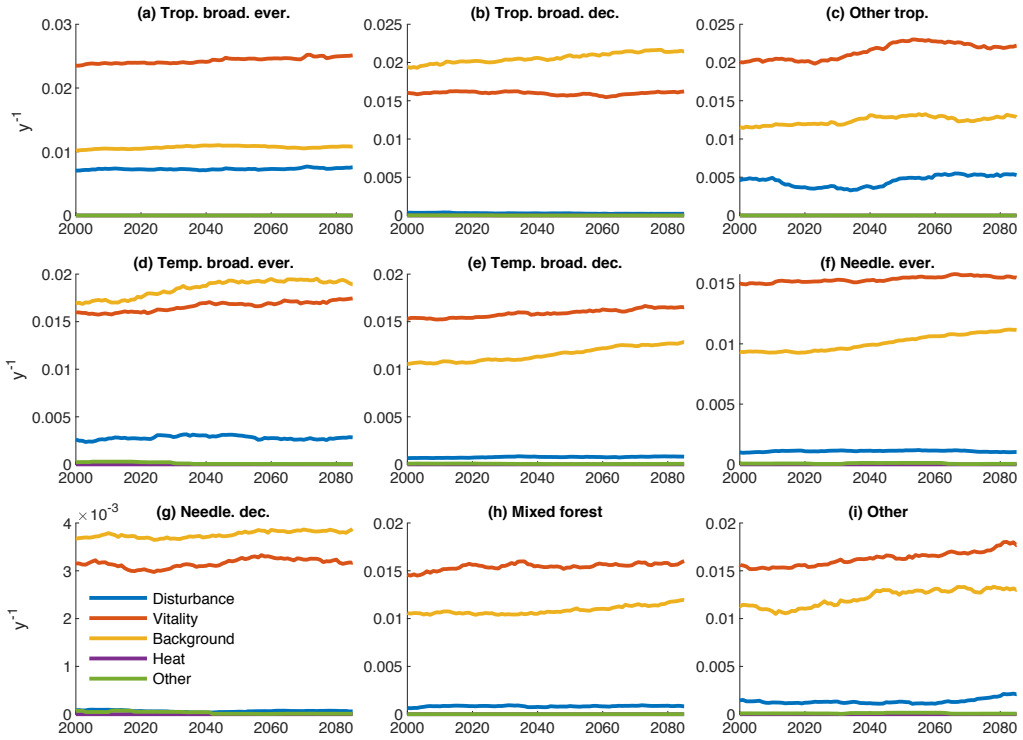

Figure S16. Mortality rate (F_{mort}/C_{veg}) for SEIB-DGVM split by conceptual process grouping (Table 3) and observational forest type for 1985-2099 in the simulation forced by IPSL-CM5A-LR RCP 8.5 bias-corrected climate data. 31-year running means are plotted for clarity and thus only 2000-2085 is shown. Rates are calculated based on grid-cell total C_{veg} and mortality fluxes.

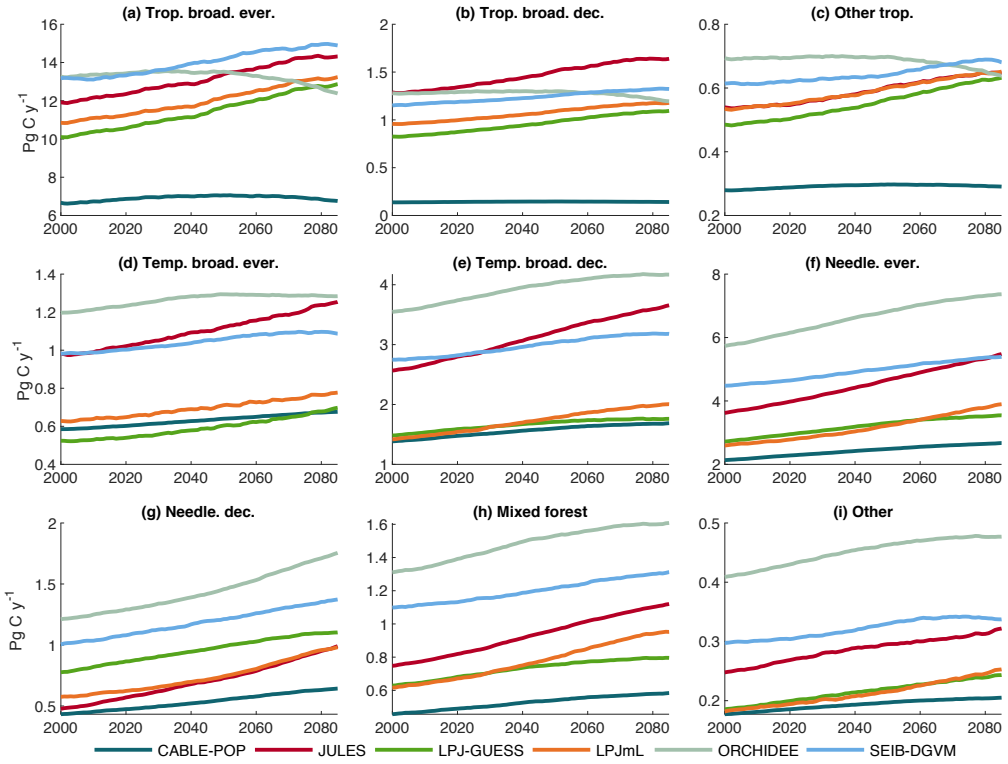

Figure S17. Change in NPP sums by observational forest type for 1985-2099 in the simulation forced by IPSL-CM5A-LR RCP 8.5 bias-corrected climate data. 31-year running means are plotted for clarity and thus only 2000-2085 is shown.

References

Clark, D. B., Mercado, L. M., Sitch, S., Jones, C. D., Gedney, N., Best, M. J., Pryor, M., Rooney, G. G., Essery, R. L. H., Blyth, E., Boucher, O., Harding, R. J., Huntingford, C. and Cox, P. M.: The Joint UK Land Environment Simulator (JULES), model description – Part 2: Carbon fluxes and vegetation dynamics, Geosci. Model Dev., 4(3), 701–722, doi:10.5194/gmd-4-701-2011, 2011.

ESA: ESA CCI Land Cover dataset (v 2.0.7), [online] Available from: http://maps.elie.ucl.ac.be/CCI/viewer/ (Accessed 29 June 2017), 2017.

Hansen, M. C., Potapov, P. V, Moore, R., Hancher, M., Turubanova, S. A., Tyukavina, A., Thau, D., Stehman, S. V, Goetz, S. J., Loveland, T. R., Kommareddy, A., Egorov, A., Chini, L., Justice, C. O., and Townshend, J. R. G.: High-resolution global maps of 21st-century forest cover change., Science, 342, 850–853, https://doi.org/10.1126/science.1244693, 2013.

Pugh, T. A. M., Arneth, A., Kautz, M., Poulter, B., and Smith, B.: Important role of forest disturbances in the global biomass turnover and carbon sinks, Nat. Geosci., 12, 730–735, https://doi.org/10.1038/s41561-019-0427-2, 2019a.

Pugh, T. A. M., Lindeskog, M., Smith, B., Poulter, B., Arneth, A., Haverd, V., and Calle, L.: The role of forest regrowth in global carbon sink dynamics, Proc. Natl. Acad. Sci. U. S. A., 116(10), 4382–4387, https://doi.org/10.1073/pnas.1810512116, 2019b.